Fatigue Strength Improvement of Lap Joints of Thin Steel Plate Using Low-Transformation-Temperature Welding Wire

A 150% increase in fatigue limit could be realized by inducing compressive residual stress in the as-welded condition

BY A. OHTA, K. MATSUOKA, N. T. NGUYEN, Y. MAEDA, AND N. SUZUKI

ABSTRACT. The fatigue strength of lap joints of thin steel plate was improved by using a developed low-transformation-temperature welding wire that induced the compressive residual stress around a welded part in the as-welded condition. The transformation of weld metal from austenite to martensite began around 180°C and finished around room temperature. This expansion of weld metal is constrained by the surrounding base metal and induces compressive residual stress. The mean stress effect due to the compressive residual stress improved the fatigue limit approximately 1.5 times.

Introduction

The fatigue strength of welded joints is very low compared with that of the base metal. The low fatigue strength of welded joints is caused by the tensile residual stress (Refs. 1, 2) and the stress concentration (Ref. 3).

There are many ways to improve the fatigue strength of welded joints — by reducing tensile residual stress, inducing compressive residual stress, or reducing the stress concentration at fatigue-critical areas; one example is peening (Ref. 4). These methods are not able to avoid the cost and manufacturing time of postweld treatment.

Compressive residual stress can be induced without any preheating or postweld treatment by using a developed low-transformation-temperature welding wire (Ref. 5).

The improvement has already been confirmed in thick welded joints of box welds (Ref. 6), box section welded members (Ref. 7), girth welds of welded pipe (Ref. 8), and repairs of fatigue cracks initiated around box welds (Refs. 9, 10).

In this paper, the method is applied to lap joints of thin steel plate. The fatigue limit was improved by a magnitude of about 1.5 times by the stress ratio effect due to compressive residual stress induced in the as-welded condition.

A. OHTA, Y. MAEDA, and N. SUZUKI are with the National Institute for Materials Science, Ibaraki, Japan. K. MATSUOKA is with the National Maritime Research Institute, Tokyo, Japan. N. T. NGUYEN is with ETRS Pty Ltd, Mulgave, Victoria, Australia.

Mechanism of Inducing Compressive Residual Stress

The variations of strain or stress during the cooling process were measured on an electrohydraulic testing machine. Four-mm-diameter round bars were heated by direct electric current and cooled with Ar gas. The temperature was measured by a platinum/platinum-rhodium thermocouple bonded by percussion welding. The strain of the longitudinal axis, ε_y, was measured or controlled with an extensometer; the stress on the cross-section area, σ_y, was measured with a load cell.

Figure 1 shows the variation of ε_y during the cooling process. In the case of conventional welding wire, shrinkage is dominant, though a small expansion occurs around 500°C due to the transformation from austenite to martensite. Therefore, tensile residual stress is induced at room temperature when the strain is constrained, as shown in Fig. 2.

However, in the case of low-transformation-temperature welding wire, expansion dominates, as shown in Fig. 1, because the transformation finishes around room temperature. So compressive residual stress is induced, as shown in Fig. 2. It is significant that compressive residual stress can be induced in the as-welded condition. That is, compressive residual stress is induced without any postweld treatment.

KEY WORDS

Fatigue Strength
Welded Joint
Transformation
Residual Stress
Improvement
Welding Wire
Steel

Calculation of Estimated Residual Stress

It is possible to calculate (Ref. 11) that the compressive residual stress is induced in a T-joint of thin steel plate even in the case of conventional welding wire.

If the compressive residual stress is induced in a lap joint of thin steel plate made with conventional welding wire, the improvement effect could not be predicted. Therefore, the residual stress distribution around the welded part of the lap joint is estimated by using the inherent stress method and the finite element method (FEM).

Figure 3 shows the mesh division for FEM calculation. The calculation was done by fixturing both edge parts of a 100-mm-long joint. The length of fixturing was 27.5 mm for both sides. After the lap joint cooled down, the fixturing was released.

Figures 4 and 5 show the result of calculations of the residual stress distribution in the cross section at the weld toe. Figure 4 shows the results for conventional welding wire of MGS-63B, and Fig. 5 shows results for the developed low-transformation-temperature welding wire of 10Cr-10Ni. Curves are obtained under the constrained condition or under free deformation condition after the release of fixturing.

In curves under free deformation condition, the residual stress at the weld toe is tensile for the conventional welding wire, and compressive for the low-transformation-temperature welding wire.

Figure 6 shows the contour of residual stress for low-transformation-temperature welding wire. It is clear the compressive residual stress also exists at the weld root.

As stated above, the opposite results of residual stress can be calculated in a lap joint made with conventional rather than the developed 10Cr-10Ni welding wire. The improvement effect is experimentally investigated as follows.

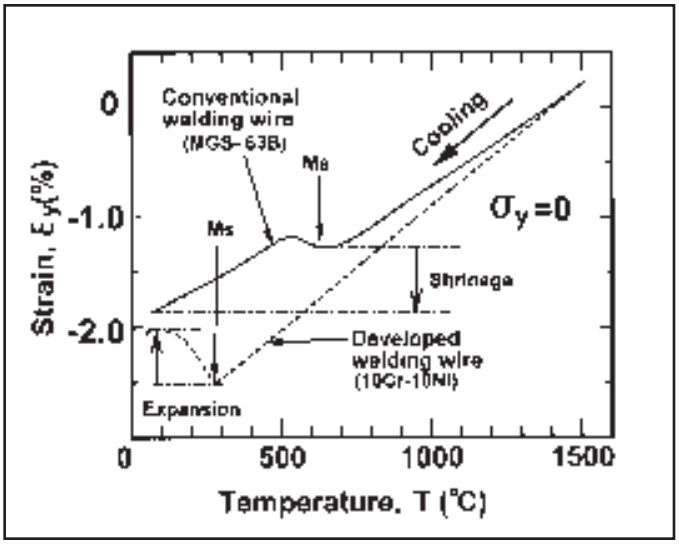

Fig. 1 — Variation of strain of weld metal during cooling process.

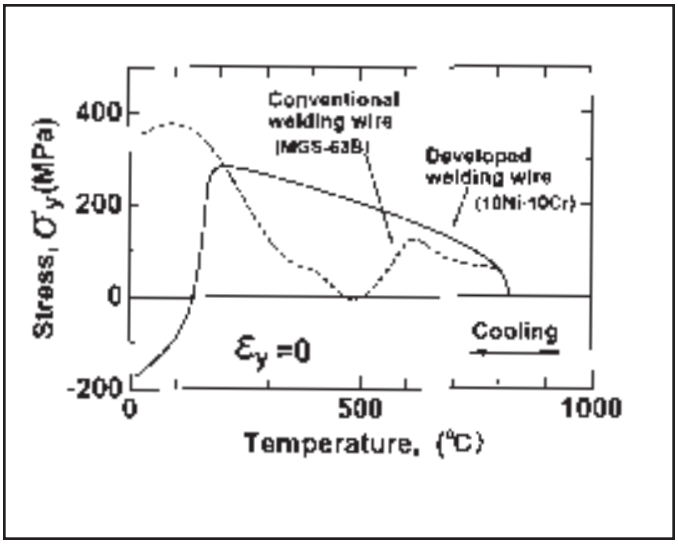

Fig. 2 — Variation of stress of weld metal during cooling process.

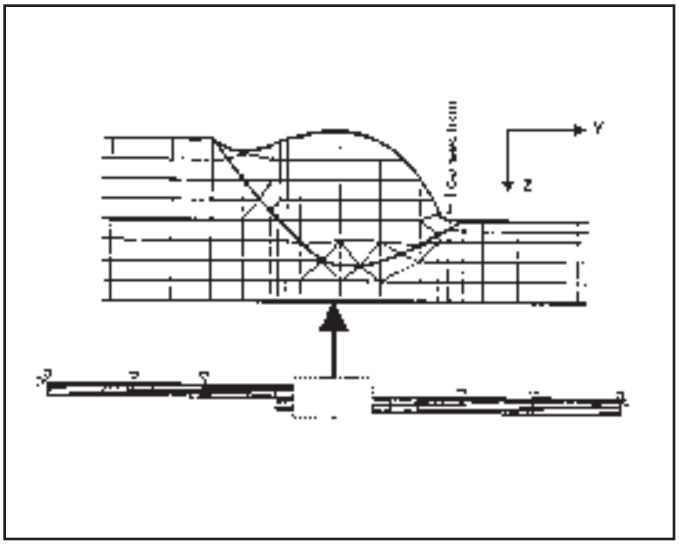

Fig. 3 — Mesh division for FEM calculation.

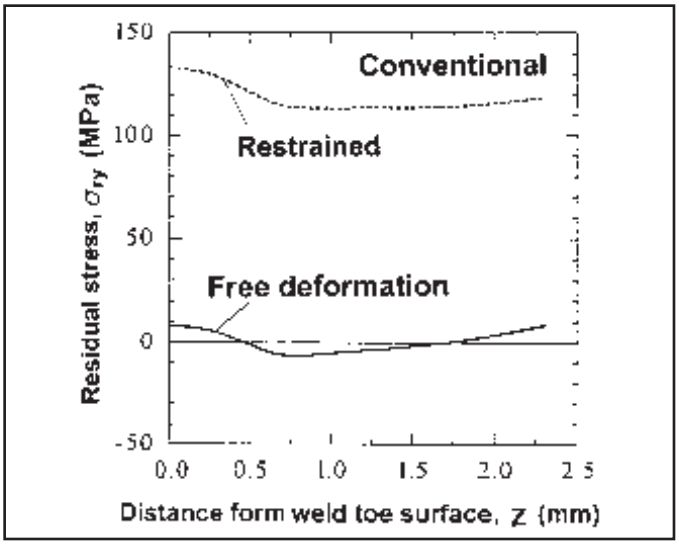

Fig. 4 — Estimated residual stress distribution for conventional welding wire welded joint.

Experimental Procedures

The thin steel plate used in this experiment is JIS SPFH 540 with a thickness of 2.3 mm. The chemical composition and mechanical properties of the plate and welding wires are shown in Tables 1 and 2, respectively.

The diameter of the welding wire is 1.2 mm. The shielding gas contains 80% Ar and 20% CO_2. The welding conditions are indicated in Table 3. These were found to be suitable for each welding wire. The differences in welding conditions resulted from differences in electrical resistance and viscosity of the wires. The welding was done using the constraining tool shown in Fig. 7. After cooldown of the joint, it was released from the tool.

Fatigue specimens for the out-of-plane bending test shown in Fig. 8 are machined from the welded joint. The cross sections of the welded specimen are shown in Fig. 9.

The residual stress perpendicular to the weld line, σ_{ry}, on the cross section of the weld toe was measured (Ref. 12) by using a strain gauge and cutting the plate surface gradually, as shown in Fig. 10A. The relationship between the strain and cut depth was drawn, and the following equations were used to obtain the residual stress. When the cutting depth reached a half-thickness of the plate, the new strain gauge was bonded on the machined surface. Then the strain of the newly bonded gauge was measured during the cutting process of the back surface — Fig. 10B. Equation 1 is used for the surface cutting process, and Equation 2 for the back surface cutting process.

$$\sigma_1 = E\left\{2\varepsilon - \frac{t-z}{2}\frac{d\varepsilon}{dz} - 3(t-z)\int_0^z \frac{\varepsilon}{(t-z)^2}dz\right\} \quad (1)$$

$$\sigma_2 = E\left\{\begin{array}{l} 2\varepsilon' - \dfrac{t-2z'}{4}\dfrac{d\varepsilon}{dz'} - \\ 3\left(\dfrac{t}{2}-z'\right)\displaystyle\int_0^{z'}\frac{\varepsilon'}{\left\{\left(\frac{t}{2}\right)-z'\right\}^2}dz' \end{array}\right\} + \frac{3E}{1-\upsilon^2}\left(\frac{t}{4}-z'\right)\left\{\int_0^{\frac{t}{2}}\frac{\varepsilon}{(t-z)^2}dz - \frac{2}{t}\varepsilon'_{t/2}\right\} - \frac{2}{t}\int_0^{\frac{t}{2}}\sigma_1 dz \quad (2)$$

where E is Young's modulus; υ is Poisson's

ratio; ε is the strain measured when the surface layer was cut to depth z; t is the original plate thickness; ε' is the strain measured when the back surface layer of the remaining half thickness was cut to depth z'; and $\varepsilon'_{t/2}$ is the strain measured when the plate was cut to depth ½— Fig. 10C.

Fatigue tests were done on an electro-hydraulic machine having a 2-kN load cell in ambient air. The four-point bending device was attached on the machine. The waveform was sinusoidal, the test frequency was 3.5 Hz, and the stress ratio was 0.

The beach mark tests were performed on some specimens by reducing the stress amplitude by half, keeping the maximum stress. The full-stress amplitude and half-stress amplitude loading were repeated periodically. In the beach mark tests, the number of cycles to failure on the S-N diagram was regarded to be the sum of the number of cycles corresponding to the full-stress amplitude. That is, the number of cycles corresponding to the half-stress amplitude was neglected.

The strain amplitude was measured during fatigue testing with a strain gauge bonded at the distance of 3 mm from the weld toe.

Results and Discussions

Figure 11 shows the measured residual stress distribution. In the case of a conventional joint made with conventional MGS-63B welding wire, tensile residual stress is induced near the weld toe. However, in the case of a joint made with the

Table 1 — Chemical Composition of Materials

		Chemical composition (wt-%)								
		C	Si	Mn	P	S	Ni	Cr	Mo	Fe
Base metal	SPFH590	0.03	0.70	1.14	0.012	0.001	—	—	—	Balance
	Requirement	—	—	—	—	—	—	—	—	
Welding material	MGS-63B	0.08	0.50	1.09	0.007	0.008	—	0.42	0.29	Balance
	10Cr-10Ni	0.025	0.32	0.70	—	—	10.0	10.0	0.13	Balance
	Requirement of YCW24	≤ 0.15	—	—	≤ 0.025	≤ 0.025	—	—	—	Balance

Table 2 — Mechanical Properties of Materials

		Mechanical properties				
		Yield strength (MPa)	Tensile strength (MPa)	Elongation (%)	Hardness Hv	Impact value (J/°C)
Base metal	SPFH590	557	680	20	171	—
	Requirement	≥ 420	≥ 590	≥ 20	—	—
Welding material	MGS-63B	580	660	29	272	150/–20
	10Cr-10Ni	822	1192	26	397	39/–20
	Requirement of YCW24	≥ 490	≥ 570	≥ 19	—	≥ 27/–20

Table 3 — Welding Condition

Welding wire	Welding current	Arc voltage	Welding speed	Heat input	Shielding gas
MGS-63B	150A	18V	75cm/min	2.2kJ/cm	80%Ar+20%CO_2/2.5L/min
10Cr-10Ni	170A	22V	70cm/min	3.2kJ/cm	80%Ar+20%CO_2/2.5L/min

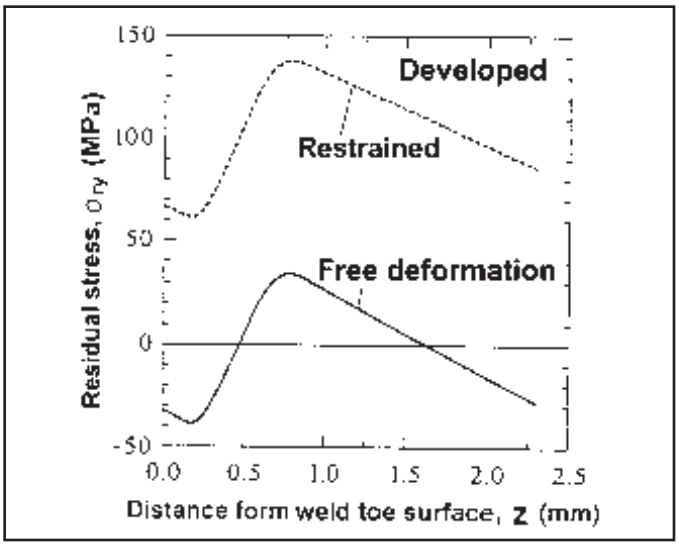

Fig. 5 — Estimated residual stress distribution for developed welding wire welded joint.

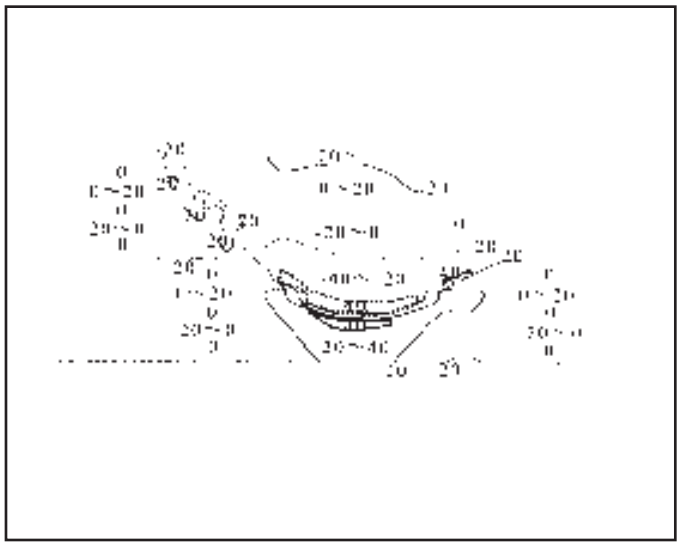

Fig. 6 — Contour of residual stress for developed welding wire welded joint.

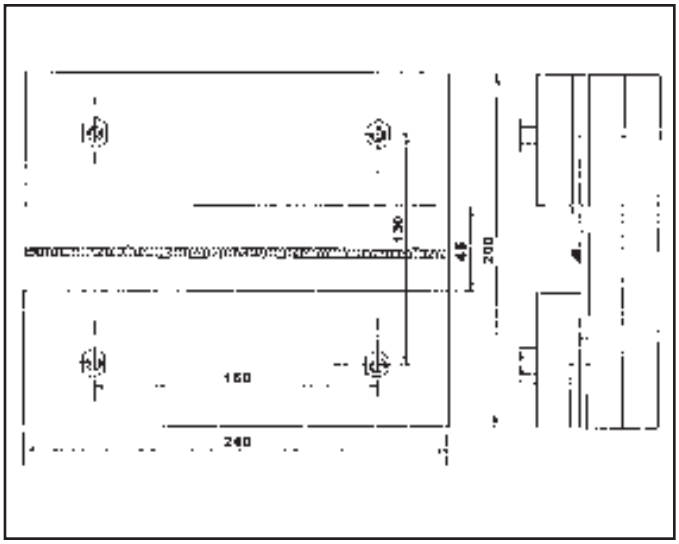

Fig. 7 — Constraining tool for welding of lap joints.

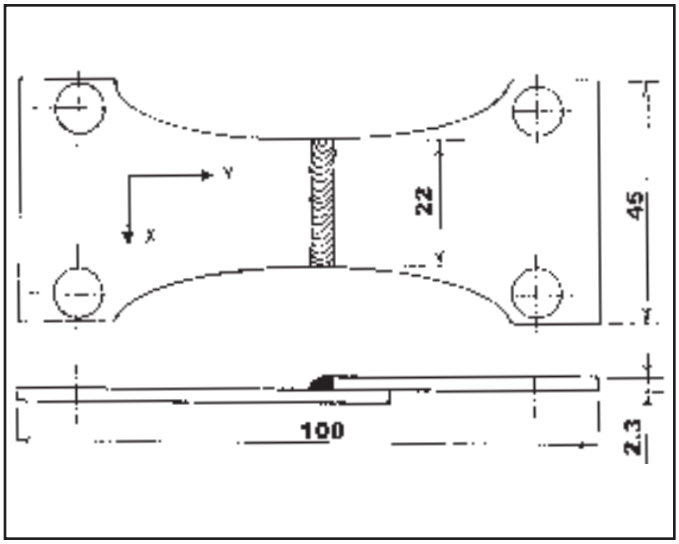

Fig. 8 — Fatigue specimen.

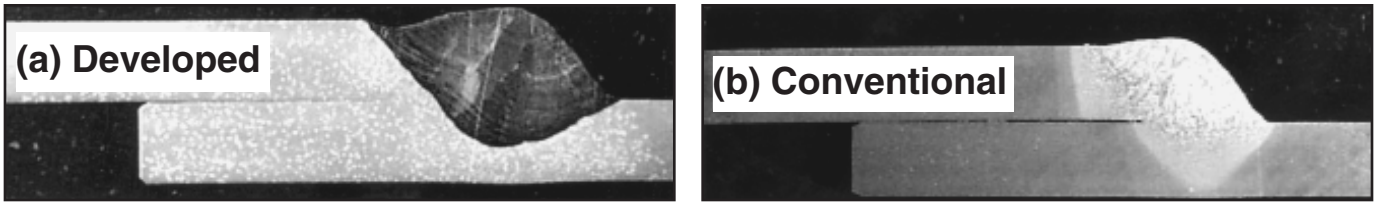

Fig. 9 — Macrostructure of lap joints.

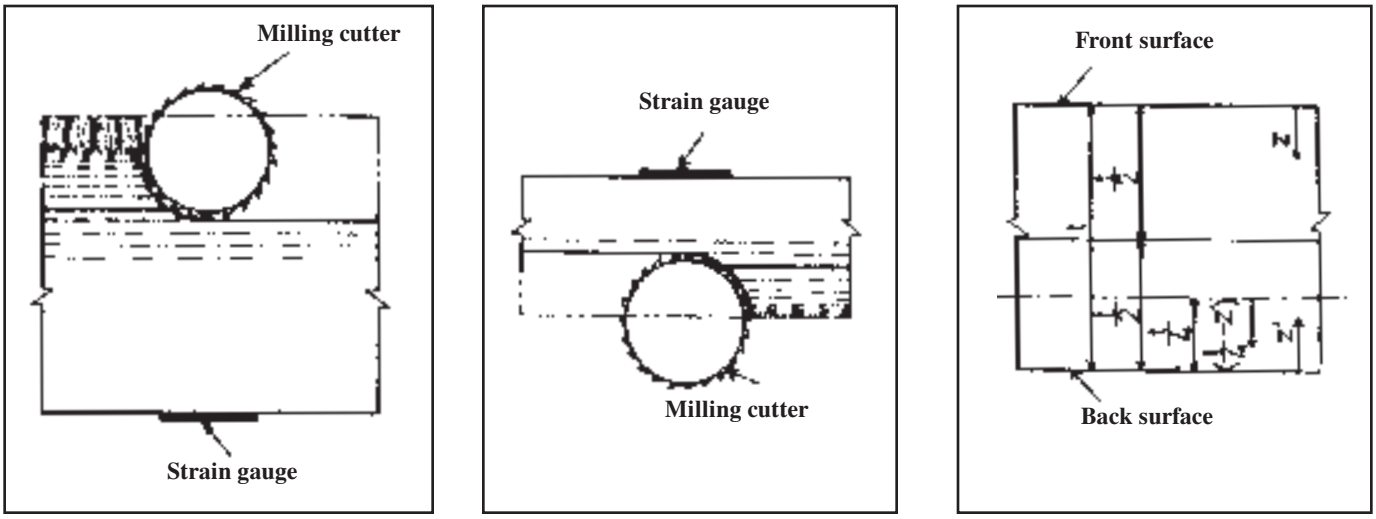

Fig. 10 — Procedure for measuring residual stress with plate thickness.

developed 10Cr-10Ni welding wire, compressive residual stress is induced near the weld toe. The trends of residual stress distribution are similar to those of the calculations shown in Figs. 4 and 5. However, the magnitude of residual stress is different. The difference occurs from the inherent stress function that is usually used for thick welded plate. In this experimental work, the plate thickness is thin and the cooling rate is quite different. This difference of cooling rate controls the inherent stress function. That is the reason for the difference in magnitude of residual stress between the calculations and measurements. The similar trends of residual stress distribution show that the degree of residual stress in thin plate can be estimated by the inherent stress function for thick plate.

The beach marks on the fracture surface are shown in Fig. 12. The fatigue cracks initiated from the weld toe for both types of joints. In the case of conventional welding wire of MGS-63B, the beach marks are shallow. That means the fatigue crack easily grew along the weld toe, because the tensile residual stress near the surface assisted the fatigue crack growth in the direction of width. The number of beach marks is large, and the ratio of beach mark number to full block number in the beach mark test was larger than 0.9.

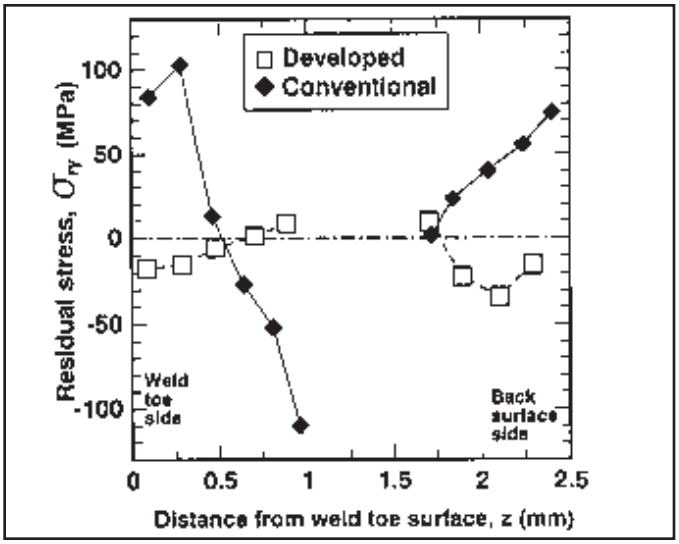

Fig. 11 — Measured residual stress distribution at weld toe section.

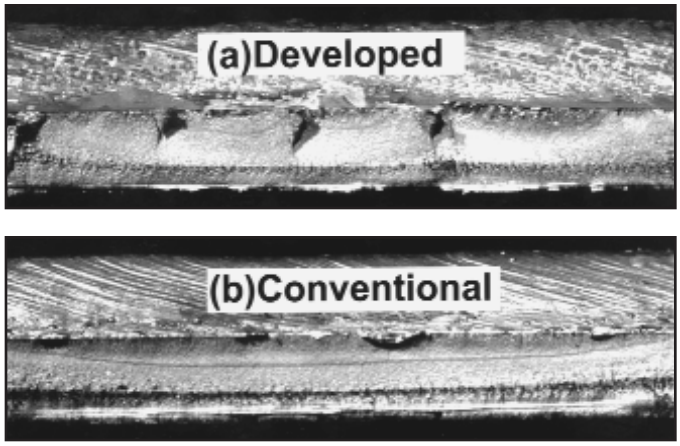

Fig. 12 — Beach marks on fractured surface.

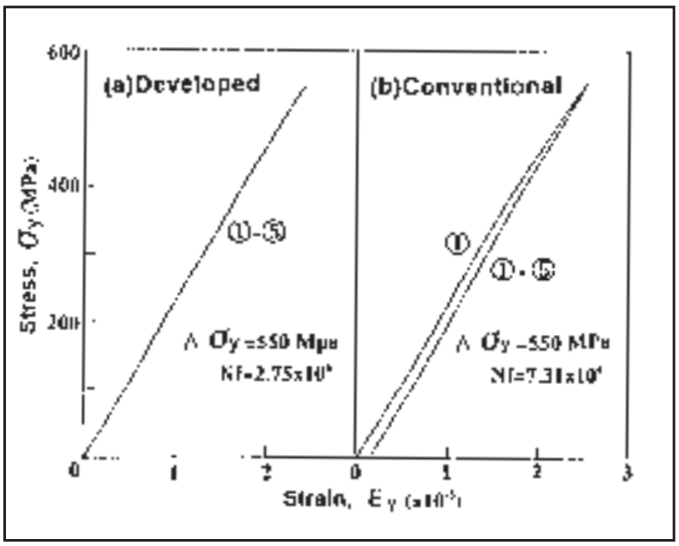

Fig. 13 — Relationship between stress and strain in early fatigue cycling.

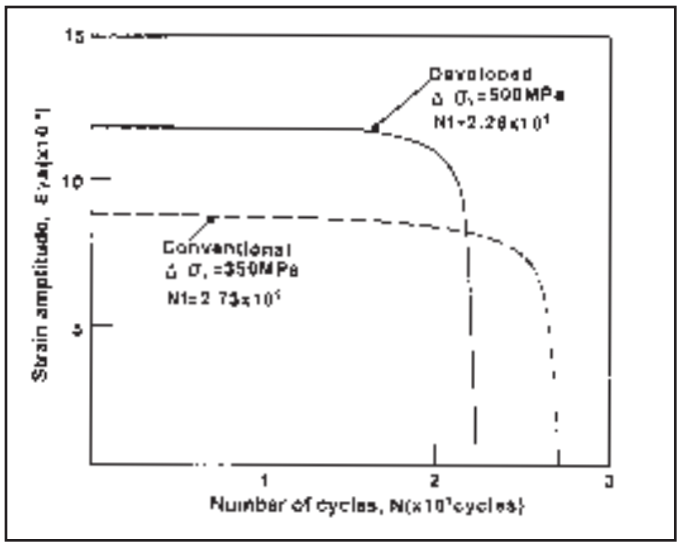

Fig. 14 — Variation of strain amplitude during cycling.

That is, the fatigue crack growth shared more than 90% of fatigue life.

In the case of the developed 10Cr-10Ni welding wire, the beach marks have a deep ellipsoidal shape, because the compressive residual stress near the surface prevented the fatigue crack growth in the width direction. The number of beach marks is small, and the ratio of beach mark number to full block number in the beach mark test was smaller than 0.3. That is, the fatigue crack growth shared less than 30% of fatigue life.

Figure 13 shows the relationship between stress and strain in the beginning period of fatigue loading. The numbers in open circles in this figure indicate the number of cycles in the fatigue test. In the case of conventional welding wire of MGS-63B, the plastic strain is observed at the first loading excursion because the tensile residual stress is added to the applied stress and the maximum stress of tensile residual stress plus applied stress easily exceeded the yield strength of the material. The relationship for later cycles, after two cycles, is almost elastic.

But in the case of the developed 10Cr-10Ni welding wire, the relationship is almost elastic even for the first loading excursion because the maximum stress of compressive residual stress plus applied stress does not exceed the yield strength of the material.

The variation of strain range with cycling is shown in Fig. 14. In the case of the conventional MGS-63B welding wire, the reduction of strain range occurs gradually from the beginning of the test. This trend suggests the fatigue crack initiated in the early period of fatigue life.

But in the case of 10Cr-10Ni low-transformation-temperature welding wire, the strain amplitude does not change until a later period of the test. This trend suggests the fatigue crack initiated in the later period of fatigue life.

Figure 15 shows the S-N curves. The fatigue limit for the conventional MGS-63B welding wire is 300MPa, while the fatigue limit for the 10Cr-10Ni low-transformation temperature-welding wire is 475 MPa. The increase in fatigue limit for low-transformation-temperature welding wire occurs from the stress ratio effect due to the compressive residual stress around the weld toe.

In the higher stress range, the effect on the stress ratio due to compressive residual stress becomes small. When the stress range reaches the yield strength of the material, the stress ratio effect due to residual stress vanishes. So the improvement effect reduces with the increase of the stress range.

In this experimental work, the loading mode was a four-point bending of R=0 for

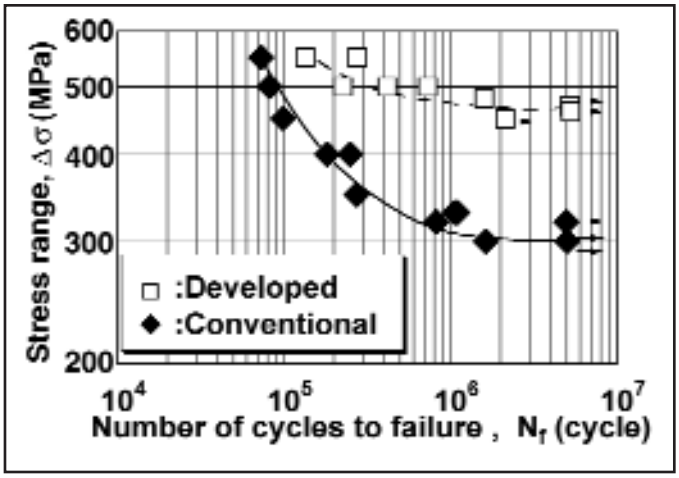

Fig. 15 — S-N curves.

inducing tensile stress at the weld toe. This type of loading is very favorable for the improvement effect. There may be other types of loading, for example, opposite side of bending moment, which induce compressive stress at the weld toe, or tension loading of R>0.5. The improvement effects for this joint with these loading types need to be investigated prior to the application of the developed 10Cr-10Ni welding wire in a real structure.

Conclusions

Lap joints of thin steel plate were made with 10Cr-10Ni low-transformation-temperature welding wire, which expands at around room temperature due to transformation from austenite to martensite.

Compressive residual stress could be induced around the weld toe in the as-welded condition by using this welding wire.

The fatigue limit at the stress ratio of 0 under out-of-plane bending was improved from 300 to 475 MPa due to the stress ratio effect of compressive residual stress when the fatigue crack initiated at the weld toe.

References

1. Fisher, J. W. 1971. Fatigue strength of welded A514 steel beams. *Proc. Conference on Fatigue of Welded Structures* Cambridge: The Welding Institute, 1:135–148.

2. Ohta, A., Sasaki, S., Inagaki, M., Kamakura, M., Nihei, M., and Kosuge, M. 1981. Effect of residual stresses on threshold level for fatigue crack propagation in welded joints of SM50B steel. *Trans. of Japan Welding Society* 50: 31–38.

3. Sanders, W. W., Decerecho, A. T., and Munse, H. 1965. Effect of internal geometry on fatigue behavior of welded joints. *Welding Journal* 44(2): 49-s to 55-s.

4. Polmear, I. J. 1979. Effect of peening on the fatigue performance of aluminum alloy fillet welds. *Metallugical Forum* 2: 20–28.

5. Ohta, A., Watanabe, O., Matsuoka, K., Shiga, T., Nishijima, S., Maeda, Y., and Suzuki, N. 1999. Fatigue strength improvement by using newly developed low transformation temperature welding material. *Welding in the World* 43: 38–42.

6. Ohta, A., Maeda, Y., and Suzuki, N. 2000. Fatigue strength improvement by using developed low transformation temperature welding wire and PWHT. *Welding in the World* 44: 52–56.

7. Ohta, A., Maeda, Y., Nguyen, T. N., and Suzuki, N. 2000. Fatigue strength improvement of box section beam by low transformation temperature welding wire. *Welding in the World* 44: 26–30.

8. Ohta, A., Maeda, Y., and Suzuki, N. 2000. Fatigue strength improvement of butt welded pipe by using low-temperature-transformation welding material. *Preprint of National Conference of Japan Welding Society* 66: 120–121 (in Japanese).

9. Ohta, A., Maeda, Y., and Suzuki, N. 2001. Fatigue life extension by repairing fatigue cracks initiated around box welds with low transformation temperature welding wire. *Welding in the World* 45: 3–8.

10. Ohta, A., Suzuki, N., and Maeda, Y. Extension of fatigue life by additional welds around box welds using low transformation temperature welding material. Submitted for publication to the American Society of Civil Engineers.

11. Matsuoka, K., Takahasi, I., Yoshii, T., and Fujii, E. 1993. Influence of residual stress on fatigue strength of non-load-carrying fillet welded joints. *Trans. of Japan Welding Society.* 24: 70–77 (in Japanese).

12. Kawada, Y., Taira, S., and Tada, Y., 1972. *Manual for Stress Measurements,* 363–366. Tokyo: Ohm Press (in Japanese).